ELSEVIER

Global and Planetary Change 19 (1998) 19–34

GLOBAL AND PLANETARY CHANGE

The land-surface flux model PROGSURF

Ferenc Ács [a,*], Michael Hantel [b]

[a] *Eötvös Loránd University, Department of Meteorology, Ludovika tér 2, H-1083 Budapest, Hungary*
[b] *Institut für Meteorologie und Geophysik der Universität Wien, Hohe Warte 38, A-1190 Vienna, Austria*

Received 8 September 1997; accepted 9 February 1998

Abstract

The land-surface flux model (PROGSURF) designed jointly at the Universities of Vienna and Budapest is reviewed; it belongs to the broad spectrum of PILPS [1] models. PROGSURF comprises one vegetation layer and three soil layers. Temperature prediction is made by the heat conduction equation in conjunction with the force-restore method. Turbulent heat fluxes are parameterized by gradient laws using the resistance concept. The formula for the canopy surface resistance involves both a parameter describing atmospheric demand and one describing moisture availability. Soil moisture prediction is made with Richards' equation. PROGSURF is tested in off-line mode for the Cabauw data set. The observed annual mean values of the state and flux quantities at the earth's surface are well reproduced. For example, the model yields latent and sensible heat fluxes of -35.3 and -2.4 W/m^2, respectively; evapotranspiration and runoff is -449 and 326 mm/yr; and root zone soil moisture content is 0.344 m^3/m^3. Further, the seasonal changes of water and energy balance components are well simulated. The sensitivity of PROGSURF to the canopy resistance formulation is analysed. We find that the atmospheric demand is largely represented by the saturation value of the evapotranspiration/soil moisture curve with maximum summer impact upon the annual value and further that the moisture availability is represented by the slope of the evapotranspiration curve. Both saturation value and slope control the amplitude of the seasonal fluctuation of the water balance components; at Cabauw site the saturation value is the governing parameter. These results fit satisfactorily into the other PILPS models. In particular, we are able to reproduce with PROGSURF the total variability of most other PILPS models by simply changing the atmospheric demand and soil moisture availability parameters. PROGSURF presently serves to simulate observed surface fluxes for an atmospheric diagnostic model.

Keywords: force-restore method; canopy resistance; moisture availability; atmospheric demand; PILPS; Cabauw

1. Introduction

Land-surface schemes (LSS) serve as subroutines in different atmospheric, hydrological and ecological models. The various existing LSS differ widely in structure and parameterization. The *Project for Intercomparison of Land-surface Parameterization Schemes* (PILPS), which is part of the *World Climate Research Programme* (WCRP) under the auspices of the *Global Energy and Water Cycle Experiment* (GEWEX) and the *Working Group on Numerical Experimentation* (WGNE) tends to improve the understanding of LSS with respect to their structural and parameterization differences.

The objectives of PILPS have been presented (Henderson-Sellers et al., 1993) and its various

* Corresponding author.

[1] Project for Intercomparison of Land-surface Parameterization Schemes.

0921-8181/98/$ - see front matter
PII: S0921-8181(98)00039-3

phases have been reviewed before (Henderson-Sellers et al., 1995). Specifically, PILPS has conducted a number of sensitivity studies. LSS with different structure and parameterizations were compared in diverse climatic conditions, e.g., at Caumont in Southern France (Henderson-Sellers, 1996) at Cabauw in the Netherlands (Chen et al., 1997) or at Valdai in Russia (Schlosser et al., 1997). These studies showed that there was considerable scatter between the PILPS models; further, it was impossible to establish a link between the model's performance and the responsible mechanisms because most LSS differed in various aspects simultaneously (Shao and Henderson-Sellers, 1996).

In the present study, we introduce a new PILPS-type model referred to as PROGSURF (**Prog**nosis of **Sur**face **F**luxes). The main purpose for yet another LSS is that we are needing a substitute for surface flux measurements as input for an atmospheric diagnostic model (Haimberger et al., 1995). Thus, we originally intended to use the *Penman–Monteith* (PM) approach (Monteith, 1965; Shuttleworth and Wallace, 1985; Dolman, 1993; Monteith, 1995) However, the routine availability of net radiation, which is the prerequisite for diagnostic application of the PM-approach, cannot be guaranteed in practice. Also, winter application would not have been possible because snow and soil freezing/melting processes cannot be simulated with the PM-approach. For these reasons we have implemented in PROGSURF aerodynamic formulae for turbulent flux parameterization.

Most ingredients of PROGSURF are standard. Emphasis is on the water budget comprising a total of four layers (vegetation plus three soil layers). Central parameterization is designed around the canopy surface resistance notion. This involves two types of conductances: one describing the *atmospheric demand* (stress function F_{ad}); and one describing the *moisture availability* (stress function F_{ma}). The effect of the atmospheric forcing (radiation, air humidity and temperature) upon stomatal functioning is condensed into F_{ad}. The availability of moisture in the soil for evapotranspiration is represented by F_{ma}.

We shall address the sensitivity issue by studying two different formulations for F_{ad}: the first is the full parameterization, the second is simply $F_{ad} = 1$. Likewise, we study two different parameterizations for F_{ma}: one with soil moisture content and one with leaf water potential. Four combinations are possible with these two parameterizations; the most complete combination (F_{ad} full, F_{ma} via leaf water potential) will be the standard setting of PROGSURF.

The aim of this study is therefore fourfold. First, we document the essential ingredients of PROGSURF. Second, we show for the Cabauw data that the standard PROGSURF reproduces the annual mean and the annual course of observations. Third, we identify with a sensitivity experiment the relevant parameters for the performance of PROGSURF; the second and third steps together serve as a skeleton test to qualify PROGSURF as PILPS model. In a fourth step, we shall try to demonstrate that the various combinations of PROGSURF, through properly choosing the relevant parameters, can reproduce the scatter between the different PILPS models.

2. Model

PROGSURF is based on previous work of Ács et al. (1991) and Ács (1994). The prognostic variables, the energy and water balance components and the layers used in the ground surface temperature and moisture prediction are schematically presented in Fig. 1. Core of the scheme is a two-layer temperature prediction of the vegetation–ground system based on the force-restore method (Noilhan and Planton, 1989) plus a three-layer diffusion type soil moisture prediction (Sellers et al., 1986). The model structure of PROGSURF differs from SiB-type models (e.g., Ács, 1994; Xue et al., 1996; Mihailović, 1996) in the sense that PROGSURF is designed to require only a minimum of soil-vegetation parameters as input. The vegetation–ground system contains a vegetation layer and a soil surface layer; the index v refers to vegetation. The turbulent heat fluxes are parameterized using the resistance concept. PROGSURF treats also the case of frozen soil but a snow representation is presently missing. Sub-gridscale variations of surface characteristics are not considered here.

The turbulent flux parameterization of PROGSURF is schematically presented in Fig. 2. The land is subdivided into a vegetated (veg) and a non-vegetated (bare soil) part (1 − veg). The vegetated land is

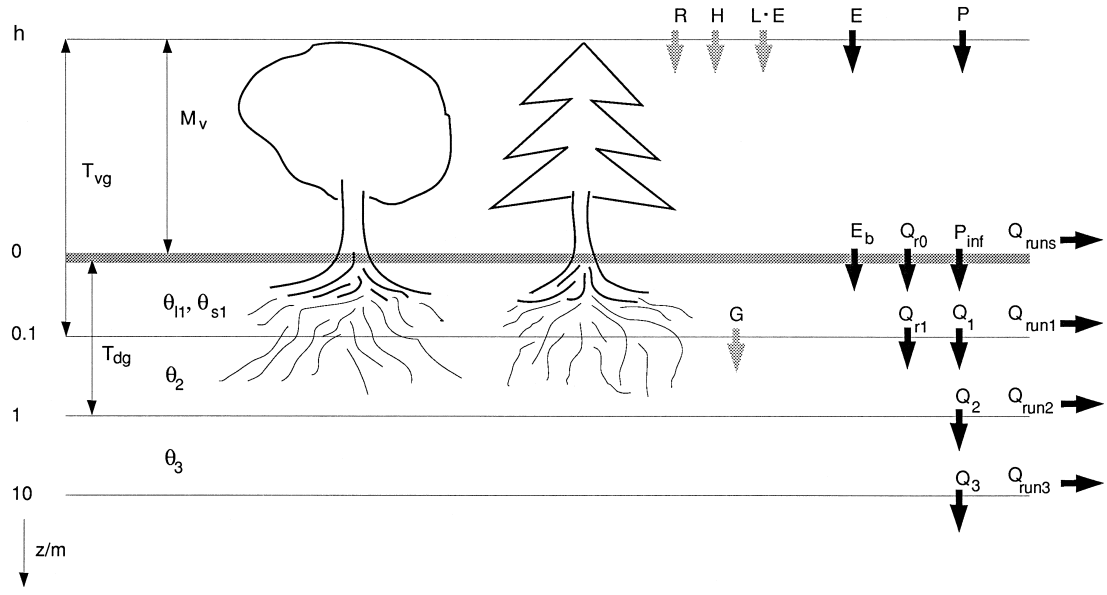

Fig. 1. Schematic diagram of prognostic variables, heat and water fluxes and layers represented by PROGSURF. Symbols for state quantities: T_{vg} = temperature of vegetation-ground layer, T_{dg} = temperature of deep-ground layer, M_v = intercepted water stored in vegetation layer, θ_{l1}, θ_{s1} = liquid and solid water content in 1st soil layer, respectively; θ_2, θ_3 = soil moisture content in 2nd, 3rd layer. Symbols for energy fluxes (in units W/m^2): R = net radiation, H = sensible heat flux, $L \cdot E$ = latent heat flux, G = soil heat flux. Symbols for water fluxes (in units kg m^{-2} s^{-1}): E = moisture flux, E_b = bare soil evaporation, P = precipitation, Q_{r0}, Q_{r1} = root water flux across surface and across bottom of 1st layer; P_{inf} = soil water flux across surface (infiltration); Q_1, Q_2, Q_3 = soil water flux across bottom of 1st, 2nd and 3rd layer; Q_{runs}, Q_{run1}, Q_{run2}, Q_{run3} = runoff from surface, 1st, 2nd and 3rd soil layer. Heat fluxes shaded, water fluxes black. All fluxes positive into positive z-direction (downward).

again subdivided into a wet vegetation (wif) and a dry vegetation part (1 − wif). Each of these subtypes are individually homogeneous. The specific surface characteristics are expressed via aerodynamic and surface resistances.

In PROGSURF, we follow the convention to count all vertical fluxes positive if directed downwards. The consequence is that, e.g., evaporation and transpiration are practically always negative. Also, the terms *vegetation* and *canopy* will be used synonymously.

2.1. Prognostic equations

The scheme has seven prognostic variables (see state quantities in left part of Fig. 1): temperature of vegetation–ground layer T_{vg}, temperature of deep-ground layer T_{dg}, intercepted water stored in vegetation layer M_v, liquid and solid water content in the 1st soil layer θ_{l1} and θ_{s1}, and soil moisture content in the 2nd and 3rd layer θ_2 and θ_3, respectively. The scheme has further a total of 16 flux quantities (right part of Fig. 1) which will be introduced consecutively.

The temperature prediction of vegetation–ground and deep-ground layers is made by using the soil heat conduction equation (Bhumralkar, 1975) and force-restore method, respectively,

$$C_B \cdot \frac{\partial T_{vg}}{\partial t} = F\left(T_{vg}, \theta_{l1}, \theta_{s1}\right) \tag{1}$$

$$\frac{\partial T_{dg}}{\partial t} = \frac{1}{\tau} \cdot \left(T_{vg} - T_{dg}\right) \tag{2}$$

where:

$$C_B = \mathrm{veg} \cdot C_v + (1 - \mathrm{veg}) \cdot C_b \tag{3}$$

$$C_b = 10\,\mathrm{cm} \cdot C + \left(\frac{\lambda \cdot C}{2\,\omega}\right)^{1/2} \tag{4}$$

$$C = (1 - \theta_{S1}) \cdot C_m + \theta_{l1} \cdot C_l + \theta_{s1} \cdot C_s \tag{5}$$

$$F\left(T_{vg}, \theta_{l1}, \theta_{s1}\right) = (R + H + L \cdot E - G) \cdot \delta\left(T_{vg}, \theta_{l1}, \theta_{s1}\right) \tag{6}$$

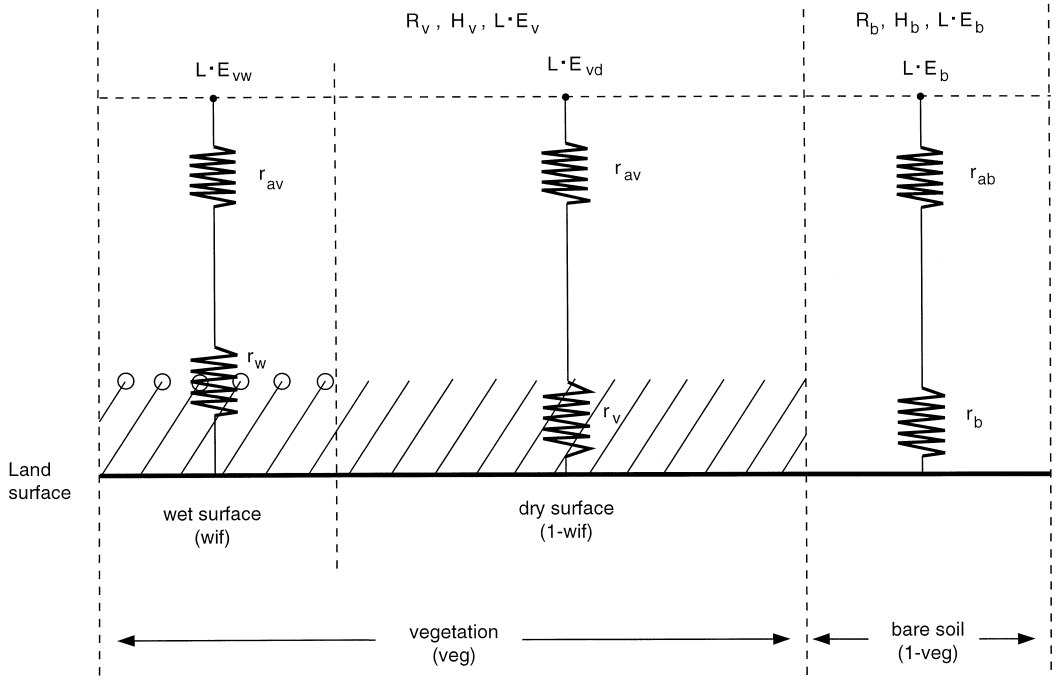

Fig. 2. Heat flux parameterization with resistance concept as implemented in PROGSURF. Symbols: R_v, H_v, $L \cdot E_v$ = net radiation, latent and sensible heat fluxes above vegetation; $L \cdot E_{vw}$ and $L \cdot E_{vd}$ = latent heat flux above wet and dry vegetation; R_b, H_b, $L \cdot E_b$: as before but for bare soil; r_{av} and r_{ab} = aerodynamic resistance above vegetation and bare soil; r_w, r_v, r_b = surface resistance of wet vegetation, dry vegetation, bare soil; wif = wet part of canopy surface; veg = vegetated part of land-surface.

The parameter C_B is the bulk heat capacity of the vegetation–ground system per unit area (in units J m^{-2} K^{-1}) with C_v, C_b = bulk heat capacity of vegetation and of the upper 10 cm of bare soil, respectively. λ is the thermal conductivity of the soil surface layer (W m^{-1} K^{-1}), ω the angular frequency of the rotation of the earth (s^{-1}). C is the volumetric heat capacity of the soil surface layer (in units J m^{-3} K^{-1}) with C_m, C_l, C_s = volumetric heat capacity of solid soil particles, water and ice, respectively. τ is the length of the day (s). For the numerical value of the constants see Table 2.

With the step function δ, the model switches between unfrozen, partly frozen and totally frozen soil as follows:

$$\delta(T_{vg},\theta_{l1},\theta_{s1}) = \begin{cases} 1 & \text{for } T_{vg} > T_{fr}, \quad \theta_{l1} \geq 0, \quad \theta_{s1} = 0 \\ 0 & \text{for } T_{vg} = T_{fr}, \quad \theta_{l1} > 0, \quad \theta_{s1} > 0 \\ 1 & \text{for } T_{vg} < T_{fr}, \quad \theta_{l1} = 0, \quad \theta_{s1} \geq 0 \end{cases} \tag{7}$$

δ regulates the temperature prediction of the vegetation–ground system. During soil freezing/melting processes, T_{vg} is equal to the freezing temperature T_{fr} and temperature prediction is switched off, represented by $F(T_{vg},\theta_{l1},\theta_{s1}) \equiv 0$. In the absence of soil freezing/melting processes, the temperature prediction of the vegetation–ground system is switched on. R, H and $L \cdot E$ are net radiation, sensible and latent heat fluxes across the surface, G is the soil heat flux across the bottom of the 1st soil layer (all energy fluxes in units W/m^2) and L is the latent heat of vaporization (J/kg).

Water storage in the vegetation layer is predicted by:

$$\frac{\partial M_v}{\partial t} = P_v - D_v + E_{vw} \tag{8}$$

where P_v is the interception of water by vegetation, D_v is the drainage of water from vegetation and E_{vw} is evaporation from wet parts of the vegetation ($E_{vw} < 0$) or dew formation ($E_{vw} > 0$).

Diffusion-type moisture prediction is applied in the soil layers. The prognostic equations for the three layers (Fig. 1) are:

$$\varrho_w \cdot D_1 \cdot \frac{\partial \theta_{l1}}{\partial t} = P_{inf} - Q_1 + Q_{r0} - Q_{r1} + E_b - Q_{run1} - S_p \quad (9)$$

$$\varrho_w \cdot D_1 \cdot \frac{\partial \theta_{s1}}{\partial t} = S_p \quad (10)$$

$$\varrho_w \cdot D_2 \cdot \frac{\partial \theta_2}{\partial t} = Q_1 - Q_2 + Q_{r1} - Q_{run2} \quad (11)$$

$$\varrho_w \cdot D_3 \cdot \frac{\partial \theta_3}{\partial t} = Q_2 - Q_3 - Q_{run3} \quad (12)$$

where ϱ_w is water density, D_i is the depth of the ith soil layer, $\theta_1 = \theta_{l1} + \theta_{s1}$, P_{inf} is the water infiltrated into the soil, E_b is the evaporation from bare soil, Q_{r0} and Q_{r1} is the root water flux across surface and across bottom of the 1st soil layer, Q_1 and Q_2 is the water diffusion between adjacent layers, Q_3 is the gravitational drainage and $Q_{run\ i}$ represents the lateral drainage from the ith layer. The gravitational and lateral drainage terms are positive representing outflow from the system. The sink term representing soil water freezing or melting is:

$$S_p = -\frac{R + H + L \cdot E - G}{L_f} \quad (13)$$

At freezing $S_p > 0$, at melting $S_p < 0$, where L_f is the latent heat of fusion (J/kg).

2.2. Radiation balance

The radiation balance of a land-surface element is written as:

$$R = S \cdot (1 - \alpha_{vg}) + \epsilon_{vg} \cdot R_a - \epsilon_{vg} \cdot \sigma \cdot T_{vg}^4 \quad (14)$$

where:

$$\alpha_{vg} = \text{veg} \cdot \alpha_v + (1 - \text{veg}) \cdot \alpha_b \quad (15)$$

S is the solar radiation and R_a is the incident atmospheric radiation, α_v and α_b is the albedo of vegetation and bare soil, respectively, ϵ_{vg} is the emissivity of vegetation and ground surface and σ is the Stefan–Boltzmann constant.

The albedo of bare soil is parameterized according to Pielke (1984). It depends upon solar zenit angle and surface wetness; the latter is estimated after Idso et al. (1975). Other factors (e.g., soil texture and color, roughness length, topography) have been neglected. Canopy albedo is analogously parameterized by an additive formula with the solar height and the surface wetness as input. The surface wetness effect is expressed via the leaf water potential using measurements of Kondratjev et al. (1982).

2.3. Heat fluxes

All turbulent fluxes apply to the top of the vegetation layer (Fig. 1). The sensible heat flux is parameterized as:

$$H_j = -\varrho c_p \frac{T_{vg} - T_r}{r_{aj}} \quad (16)$$

ϱ is the air density, c_p the specific heat of air at constant pressure, T_r a reference temperature, r_a the aerodynamic resistance. The additional index j refers to the domains of vegetation ($j = v$) with relative coverage veg, and of bare soil with coverage 1-veg ($j = b$, see Fig. 2). Thus the horizontal mean sensible heat flux is:

$$H = \text{veg} \cdot H_v + (1 - \text{veg}) \cdot H_b \quad (17)$$

Similarly the latent heat flux is parameterized as:

$$L \cdot E_j = \frac{\varrho c_p}{\gamma} \frac{f_j \cdot e_S(T_{vg}) - e_r}{r_{aj} + r_j} \quad (18)$$

γ is the psychometric constant, $e_S(T_{vg})$ is the saturation vapor pressure at T_{vg}, e_r is the vapor pressure at reference level, r_{aj} is as before, r_j is surface resistance. The index $j = b$ is for bare soil as before; f_b is the relative humidity of air at bare soil surface. For vegetation, we additionally distinguish between wet ($j = vw$) and dry ($j = vd$). In both cases, we put $f_{vw} = f_{vd} = 1$; the wet/dry distinction applies only to the surface resistance r_j. Thus, the horizontal mean latent heat flux is:

$$L \cdot E \text{ with } E = \text{veg}[\text{wif} \cdot E_{vw} + (1 - \text{wif}) \cdot E_{vd}] + (1 - \text{veg}) E_b \quad (19)$$

For simplicity, the vegetation resistances r_{vw}, r_{vd} will be abbreviated as r_w, r_v, respectively. wif is parameterized after Sellers et al. (1986), f_b after Noilhan and Planton (1989).

The soil heat flux is parameterized as:

$$G = \left(\frac{\omega \cdot C_B \cdot \lambda}{2} \right)^{1/2} \left(T_{vg} - T_{dg} \right) \tag{20}$$

This formula fits into the force-restore method (Bhumralkar, 1975) implemented in PROGSURF (Noilhan and Planton, 1989) by coupling Eqs. (1) and (2). The parameter λ is parameterized after McCumber and Pielke (1981).

2.4. Water fluxes

The water transport processes in the soil–vegetation–atmosphere system comprises interception, drainage, infiltration and surface runoff, root water fluxes, evapotranspiration, conductance of water through roots and stems and subsurface runoff. Parameterizations of these processes will now be briefly reviewed.

2.4.1. Water transfer in the soil

The water flux P_o through the soil surface is the sum of rainfall intensity P, of interception by vegetation P_v and of water drainage from the vegetation D_v:

$$P_o = P - P_v + D_v \tag{21}$$

Both P_v and D_v are parameterized after Sellers et al. (1986). P_o either infiltrates into the soil (P_{inf}) or runs out from the surface (Q_{runs}) depending upon wetness and soil texture characteristics. Infiltration is expressed by:

$$P_{inf} = \begin{cases} \min(P_o, K_{S1}) & \text{if } W_1 < 1 \\ 0 & \text{if } W_1 = 1 \end{cases} \tag{22}$$

where $W_1 = \theta_1 / \theta_{S1}$; θ_{S1} and K_{S1} are saturated soil moisture content and hydraulic conductivity in the 1st soil layer, respectively. Q_{runs} is parameterized taking into account both the Dunne and Horton mechanisms (Entekhabi and Eagleson, 1989).

The water flow between the adjacent soil layers is estimated by:

$$Q_i = K_{eff,i} \left\{ 2 \frac{\Psi_i - \Psi_{i+1}}{D_i + D_{i+1}} + 1 \right\} \tag{23}$$

$$K_{eff,i} = \frac{D_i \cdot K_i + D_{i+1} \cdot K_{i+1}}{D_i + D_{i+1}} \tag{24}$$

where $K_{eff,i}$ is an effective hydraulic conductivity between the ith and the $(i+1)$th ($i = 1,2$) soil layer, K_i is the hydraulic conductivity of the ith soil layer (both conductivities in units kg m^{-2} s^{-1}) and Ψ_i is the soil water potential of the ith soil layer (m). Both latter terms are parameterized after Clapp and Hornberger (1978).

Subsurface runoff is the sum of lateral and gravitational drainage. Lateral drainage is parameterized for each soil layer ($i = 1,2,3$) using the expressions

$$Q_{run\,i} = \begin{cases} Q_{rf\,i} & \text{if} \quad WF_i \le \dfrac{\varrho_w D_i}{\Delta t} (\theta_{f\,i} - \theta_i) \\ Q_{rf\,i} + WF_i & \text{if} \quad WF_i > \dfrac{\varrho_w D_i}{\Delta t} (\theta_{f\,i} - \theta_i) \end{cases} \tag{25}$$

where:

$$Q_{rf\,i} = Q_i - \min(Q_i, K_{S\,i}) \tag{26}$$

$$WF_1 = P_{inf} - Q_1 + E_b + Q_{r0} - Q_{r1} - Q_{rf1} \tag{27}$$

$$WF_2 = Q_1 - Q_2 + Q_{r1} - Q_{rf2} \tag{28}$$

$$WF_3 = Q_2 - Q_3 - Q_{rf3} \tag{29}$$

where Δt is the time step used, θ_i and $\theta_{f\,i}$ is the actual and field capacity water content in the ith soil layer, respectively, WF_i represents the net water flux in the ith soil layer and $K_{S\,i}$ is the saturated hydraulic conductivity in the ith soil layer. The gravitational drainage rate from the bottom is calculated by:

$$Q_3 = K_{S3} \cdot W_3^{2B_3+3} \tag{30}$$

W_3 is defined equivalently to W_1 in Eq. (22).

2.4.2. Water transfer through vegetation

The root water flux Q_{r0} across the surface is assumed to flow in the stems of trees. We equate it to the transpiration (dry vegetation surface fraction in Fig. 2):

$$Q_{r0} = \text{veg} \cdot (1 - \text{wif}) \cdot E_{vd} \tag{31}$$

Table 1
Monthly values of fractional vegetation cover veg, leaf area index LAI and green leaf fraction GLF

	I	II	III	IV	V	VI	VII	VIII	IX	X	XI	XII
veg	0.92	0.93	0.94	0.95	0.97	0.98	0.99	0.98	0.97	0.96	0.95	0.93
LAI	0.8	1.0	1.1	1.3	1.6	1.8	1.8	1.6	1.5	1.1	1.0	0.9
GLF	0.85	0.88	0.89	0.91	0.92	0.93	0.83	0.86	0.67	0.81	0.79	0.77

The root water flux Q_{r1} across the bottom of the 1st layer is estimated as a prespecified percentage of the flux across the earth's surface:

$$Q_{r1} = 0.3 \cdot Q_{r0} \quad (32)$$

The parameterization (32) is equivalent to specifying the root water flux divergence in the surface layer.

Q_{r0} is parameterized through leaf water potential Ψ_v according to van der Hornert (1948):

$$Q_{r0} = \varrho_w \frac{\Psi_v - \Psi_R + z_T}{r_R + r_P} \quad (33)$$

where Ψ_R is the soil moisture potential in the root zone, z_T is the vegetation source–sink height, r_R is

Table 2
Values of site-specific land-surface parameters belonging to PROGSURF

Name	Symbol	Value	Unit
Reference height	z_r	20	m
Roughness length of bare soil surface	z_{ob}	0.01	m
Roughness length of vegetation	z_{ov}	0.15	m
Zero plane displacement height	d	0.0	m
Minimum/maximum stomatal resistance	r_{stmin}/r_{stmax}	40/20,000	s/m
Coefficient for stomatal response to absorbed visible radiation	K_{rl}	50	W/m^2
Optimum temperature of canopy	T_o	298	K
Coefficient governing stomatal response to vapor pressure deficit	c_v	0.0238	hPa^{-1}
Coefficient governing stomatal response to air temperature	c_T	1.6×10^{-3}	K^{-2}
Sun's empirical constants for soil surface resistance	c_1, c_2, c_3	30, 3.5, 2.3	s/m, s/m, dimensionless
Emissivity of canopy–ground system	ϵ_{cg}	1.0	
Albedo of wet vegetation (criterion: leaf water potential > -150 m)	α_{vw}	0.25	
Albedo of wet vegetation for visible part of global radiation	α_{vpw}	0.15	
Albedo of dry bare soil surface	α_{bd}	0.15	
Depth of root layer	D_R	1.0	m
Root cross-section	rcs	3.84×10^{-7}	m^2
Root density in surface layer	R_{des}	5500	m/m^3
Plant resistance imposed by plant vascular system	r_P	2.5×10^8	s
Critical leaf water potential	Ψ_{cr}	-230	m
Maximum water storage capacity per unit LAI	S_{cm}	0.1	mm
Moisture content at field capacity	θ_f	0.370	m^3/m^3
Moisture content at saturation	θ_S	0.468	m^3/m^3
Moisture content at wilting point	θ_w	0.214	m^3/m^3
Saturated soil moisture potentials	$\Psi_{S1} = \Psi_{S2} = \Psi_{S3}$	-0.045	m
Saturated soil hydraulic conductivity	$K_{S1} = K_{S2} = K_{S3}$	3.434×10^{-6}	m/s
Clapp–Hornberger's constant	$B_1 = B_2 = B_3$	10.39	
Thickness of soil layers	D_1, D_2, D_3	0.10, 0.90, 9.00	m
Site inclination	x	0.0	deg
Volumetric heat capacity of soil	C_m	2.0×10^6	$J\,m^{-3}\,K^{-1}$
Volumetric heat capacity of water	C_l	4.2×10^6	$J\,m^{-3}\,K^{-1}$
Volumetric heat capacity of ice	C_s	1.78×10^6	$J\,m^{-3}\,K^{-1}$
Surface heat capacity of vegetation	C_v	2×10^3	$J\,m^{-2}\,K^{-1}$

the soil resistance in the root zone and r_P is the plant resistance imposed by the plant vascular system. r_P depends upon the vegetation type; its value is given in Table 2. Eq. (33) will be used below to determine Ψ_v which is required for the parameterization of stomatal resistance.

2.5. Resistances

2.5.1. Aerodynamic resistance

The aerodynamic resistance in the soil–vegetation–atmosphere system is formulated with Monin–Obukhov's similarity theory taking into account the atmospheric stability. It is split into laminar and turbulent terms distinguishing transports between momentum and heat/moisture. The resistances are separately calculated above vegetated and bare soil surfaces.

2.5.2. Canopy resistance

The resistance due to the vegetation canopy is parameterized following Jarvis (1976):

$$r_v = \frac{r_{stmin} \cdot F_{ad}}{LAI \cdot GLF \cdot F_{ma}} \tag{34}$$

where r_{stmin} is the minimum stomatal resistance at optimum environmental conditions (Table 2). LAI is the leaf area index, GLF is the green leaf fraction; it expresses the fraction of live leaves ranging between 0 and 1 (Table 1). The stress functions F_{ad} and F_{ma} represent the atmospheric demand and moisture availability effect upon stomatal functioning, respectively; they range between 0 and 1.

F_{ad} is in a multiplicative manner split into three effects:

$$F_{ad} = \frac{F_{vr}}{F_{ah} \cdot F_{at}} \tag{35}$$

where F_{vr}, F_{ah} and F_{at} expresses the influence of absorbed visible radiation, air humidity and temperature, respectively. F_{vr} is parameterized after Gates (1981), F_{ah} after Jarvis (1976) and F_{at} after Dickinson (1984).

F_{ma} is parameterized in PROGSURF via leaf water potential as (Choudhury, 1983; Sellers and Dorman, 1987; Lynn and Carlson, 1990; Ács, 1994):

$$F_{ma} = \frac{\Psi_v - \Psi_{cr}}{\Psi_{SR} - \Psi_{cr}} \tag{36}$$

where Ψ_v and Ψ_{cr} is the actual and the critical leaf water potential, respectively; at $\Psi_v = \Psi_{cr}$ the stomata are closed (depending upon vegetation type, for present value, see Table 2). The saturated soil water potential in the root zone is defined as:

$$\Psi_{SR} = \frac{D_1 \cdot \Psi_{S1} + D_2 \cdot \Psi_{S2}}{D_1 + D_2} \tag{37}$$

Combining Eqs. (18), (31), (33), (34) and (36) yields the following quadratic equation for Ψ_v:

$$a \cdot \Psi_v^2 + b \cdot \Psi_v + c = 0, \tag{38}$$

with:

$$a = r_{av} \tag{39}$$

$$b = AD \cdot (r_R + r_P) - (\Psi_R - z_T) \cdot r_{av} + A \cdot (\Psi_{SR} - \Psi_{cr}) - \Psi_{cr} \cdot r_{av} \tag{40}$$

$$c = -AD \cdot (r_R + r_P) \cdot \Psi_{cr} + (\Psi_R - z_T) \cdot \Psi_{cr} \cdot r_{av} - A \cdot (\Psi_R - z_T) \cdot (\Psi_{SR} - \Psi_{cr}) \tag{41}$$

where:

$$AD = \frac{\varrho \cdot c_p}{\gamma} \cdot \frac{1}{L \cdot \varrho_w} \cdot veg \cdot (1 - wif) \cdot \left[e_s(T_{vg}) - e_r \right], \; A = \frac{r_{stmin} \cdot F_{ad}}{LAI \cdot GLF} \tag{42}$$

The soil resistance in the root zone is expressed as:

$$r_R = \frac{\alpha_R \cdot \varrho_w}{K_R \cdot D_R} \tag{43}$$

where K_R is the hydraulic conductivity in the root zone and D_R is the root zone depth. α_R is a vegetation specific parameter for the root zone:

$$\alpha_R = \frac{V_R - 3 - 2 \cdot \log\left[V_R/(1 - V_R)\right]}{8\pi R_{det}} \tag{44}$$

where V_R is the volume of root per unit volume of soil in the root zone; it is calculated from the total root density in the root zone R_{det} and the average root cross-section rcs. R_{det} is calculated after Ger-

witz and Page (1974) when the root density in the soil surface layer R_{des} is known. R_{des} and rcs are specified in Table 2. K_R and Ψ_R are calculated as weighted mean of their components analogously to Eq. (37).

The Ψ_v value is obtained by:

$$\Psi_v = \frac{-b + [b^2 - 4 \cdot a \cdot c]^{1/2}}{2a} \quad (45)$$

The other solution gives unrealistic results.

2.6. Numerical implementation of the model

The sequence of calculations in a given time step is presented in Fig. 3. The *radiation module* calculates the net radiation of land-surface estimating separately the albedo for bare soil and vegetation. The subroutine for vegetation albedo contains three subroutines which parameterize solar height, leaf water potential and aerodynamic resistances; they are iteratively coupled to simulate the interrelationship between albedo, vegetation wetness and atmospheric stratification.

The *vegetation module* contains subroutines for turbulent heat fluxes and vegetation water fluxes. The *bare soil* module calculates only the turbulent heat fluxes; the parameterization is as in the vegetation module but without interception and drainage calculation. In case of unstable stratification, the flux/aerodynamic resistance relationship is iteratively calculated for both modules.

The soil heat flux is determined in the *ground module*; there is no difference between vegetated and non-vegetated surfaces. The next subroutine calculates infiltration and surface runoff. The last subroutine in the ground module determines all subsurface water fluxes (soil water diffusion, lateral runoff and gravitational drainage). The *soil water freezing/melting module* determines the amount of subsurface phase changes of water.

The *prognostic equations* are applied in a separate *module*. During freezing or melting, the hydraulic conductivity is put to zero and T_{vg} is kept at freezing temperature.

The numerical implementation of vegetation water storage (in PROGSURF only in form of interception), soil moisture and deep-soil temperature predic-

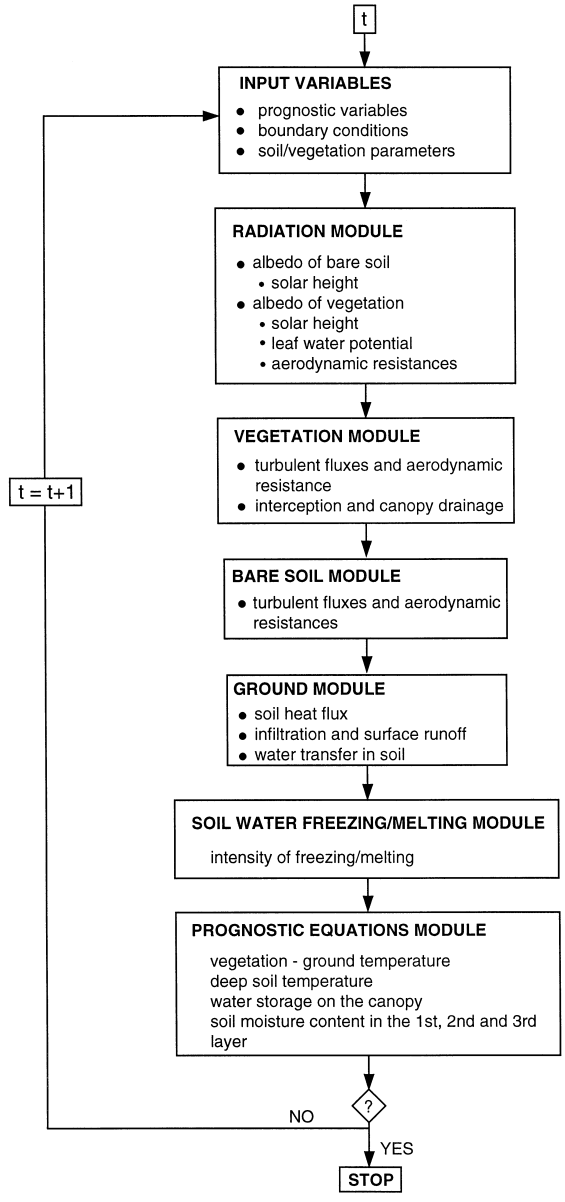

Fig. 3. Flow chart of calculations in PROGSURF in one-time step.

tion equations uses explicit time schemes. The T_{vg}-equation is solved by an implicit scheme as follows:

$$T_{vg}^{t+\Delta t} = T_{vg}^{t} + \frac{F^t}{\frac{C_B}{\Delta t} - \frac{\partial F^t}{\partial T_{vg}}} \quad (46)$$

where the derivative $\partial F^t/\partial T_{vg}$ is taken at time step

t; the function $F = F(T_{vg}, \theta_{l1}, \theta_{s1})$ has been defined above in Eq. (6). The time step used was $\Delta t = 900$ s.

3. Model validation

PROGSURF has been extensively tested in off-line mode using the 1987 data from Cabauw, Netherlands. There are three reasons for choosing the Cabauw data set: (a) the atmospheric forcing data, soil–vegetation parameters and the measured latent and sensible heat fluxes have, generally, a high quality; (b) the data series is long enough, it includes one full year which provides a basis for testing the model performance in terms of seasonal variations; and (c) the data set was mandatory for the PILPS Phase 2(a) experiment which makes it possible to compare PROGSURF with the other LSSs of the PILPS campaign. The data set has been described and analysed in detail by Beljaars and Bosveld (1997). In the numerical experiments, PROGSURF was initialized by saturating all liquid water stores and setting all temperatures to 279 K. The variable and constant land-surface parameters used are listed in Tables 1 and 2, according to the specifications of the PILPS 2(a) experiment. The surface albedo has been kept constant in PROGSURF for this experiment (see Table 2); i.e., the daily change has been neglected.

The model validation is performed here by comparing simulated (i.e., for the standard PROGSURF setting Psi1) and observed surface fluxes; this includes the annual mean characteristics of selected heat and water balance components as well as the seasonal changes and instantaneous values of net radiation and turbulent heat fluxes.

3.1. Annual mean characteristics

The annual mean characteristics refer to the equilibrium year. Equilibrium was defined as being the first occasion that the January mean values of surface radiative temperature, latent and sensible heat fluxes, and root-zone soil moisture did not change by more than 0.01 K, 0.1 W/m^2, and 0.1 mm, respectively, from year N to year $N+1$; the equilibrium year was then N years (spinup time). PROGSURF's spinup time is 2 yr.

The annual mean sensible and latent heat fluxes obtained by PROGSURF for the standard run Psi1 are presented in Fig. 4 together with the other PILPS results; the PROGSURF results for the sensitivity runs Psi2 and Theta will be discussed further below. The sensible heat flux of Psi1 is -2.4 W/m^2, the latent heat flux is about -35 W/m^2. The corresponding point in Fig. 4 is not exactly located on the radiation line; this is presumably due to T_{vg} prediction.

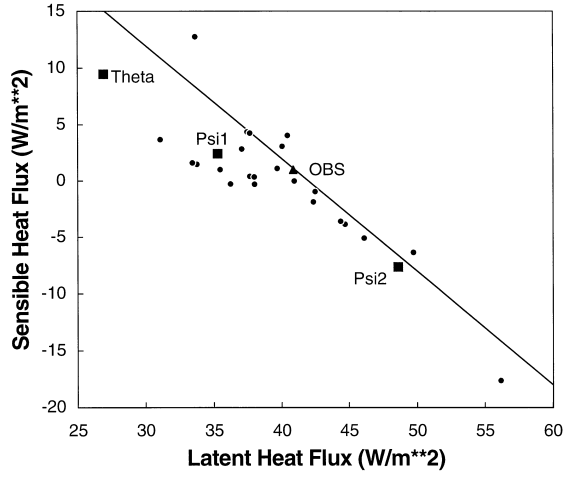

Fig. 4. Annually averaged sensible vs. latent heat fluxes estimated by the different versions of PROGSURF (thick symbols, see also text) along with the equivalent PILPS phase 2(a) results (thin dots; for details, see Fig. 5 in the paper of Chen et al., 1997). 'Psi1' = standard PROGSURF run (with F_{ad} fully parameterized and F_{ma} by leaf water potential); 'Psi2' = modified PROGSURF run with $F_{ad} \equiv 1$ and F_{ma} parameterized by leaf water potential; 'Theta' = modified PROGSURF run with F_{ad} fully parameterized and F_{ma} by soil moisture; and 'OBS' = observed value.

The annual runoff vs. evapotranspiration is given in Fig. 5. The evapotranspiration and runoff calculated by standard PROGSURF Psi1 is -449 and 326 mm/yr, respectively; the equivalent observed fluxes are -525 and 250 mm/yr, respectively. The annual mean soil water in the root zone obtained by Psi1 is 344 mm. Its estimated value (indirectly observed) is about 350 mm (Chen et al., 1997).

3.2. Seasonal variations

The seasonal change of net radiation R is presented in Fig. 6. Standard PROGSURF reproduces the observations well. The largest deviation between modeled and observed R values is about 10 W/m^2 and it appears in June.

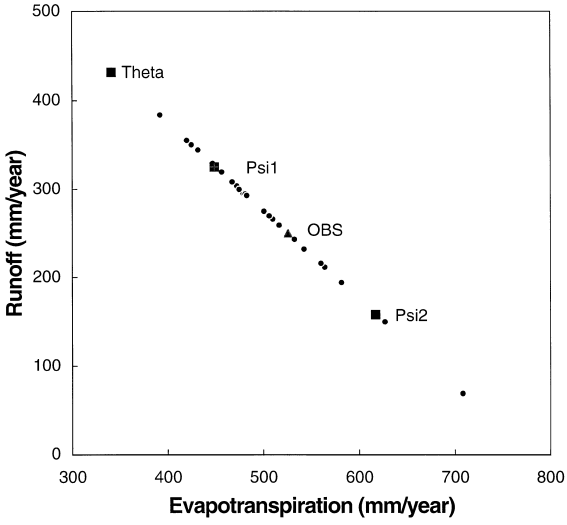

Fig. 5. As in Fig. 4 but for runoff vs. evapotranspiration (compare with Fig. 10 in the paper of Chen et al., 1997).

The seasonal change of latent and sensible heat fluxes is presented in Fig. 7. The largest deviation between simulated and observed $L \cdot E$ values is about 15 W/m^2 and it appears in May. The corresponding deviation for H is also about 15 W/m^2 but it appears in March.

3.3. Energy fluxes in the intensive observation period

Instantaneous values of net radiation and turbulent heat fluxes have been measured in the intensive observation period (IOP) between 10–19 September 1987. Simulated and observed surface net radiation during IOP is presented in Fig. 8. The slope of the regression line and the correlation coefficient are both close to 1.

The corresponding comparison for latent and sensible heat flux is presented in Figs. 9 and 10, respectively. The correlation between PROGSURF values and measured fluxes is less than for the net radiation but still sufficiently high.

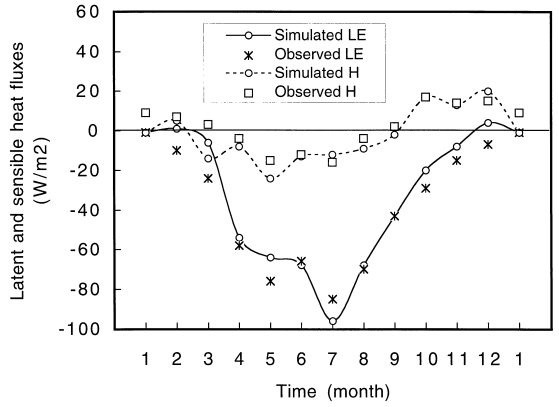

Fig. 7. Annual course of latent and sensible heat fluxes simulated by standard PROGSURF.

4. Sensitivity tests

Vegetation parameterization in PROGSURF is made with the canopy surface resistance concept. We

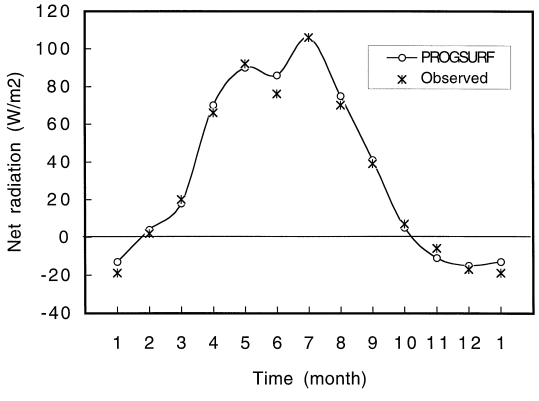

Fig. 6. Annual course of surface net radiation simulated by standard PROGSURF.

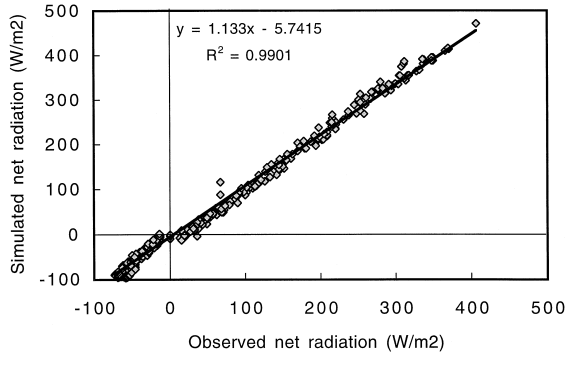

Fig. 8. Simulated (with standard PROGSURF) vs. observed surface net radiation in the IOP (from day 253 to day 262). Thick line: regression.

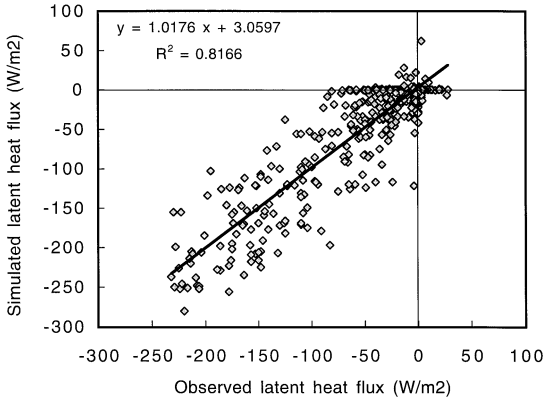

Fig. 9. Simulated (with standard PROGSURF) vs. observed latent heat flux in the IOP.

shall address the sensitivity issue by focusing on the parameters which describe atmospheric demand and moisture availability.

We consider two different formulations for F_{ad}. The first is the parameterization used in standard PROGSURF (see Eq. (35)):

$$F_{ad} = \frac{F_{vr}}{F_{ah} \cdot F_{at}} \tag{47}$$

The second is simply:

$$F_{ad} \equiv 1 \tag{48}$$

Likewise, we study two different formulations for F_{ma}. The first (standard PROGSURF, see Eq. (36)) is to parameterize it with leaf water potential:

$$F_{ma} = \frac{\Psi_v - \Psi_{cr}}{\Psi_{SR} - \Psi_{cr}} \tag{49}$$

The second is to parameterize F_{ma} via soil moisture content (Noilhan and Planton, 1989):

$$F_{am} = \begin{cases} 1 & \text{for} \quad \theta_f \le \theta \\ \dfrac{\theta - \theta_w}{\theta_f - \theta_w} & \text{for} \quad \theta_w < \theta < \theta_f \\ 0 & \text{for} \quad \theta \le \theta_w \end{cases} \tag{50}$$

where θ, θ_f and θ_w is the actual soil moisture, field capacity and wilting point soil moisture content in the root zone, respectively. There is a specific additional property of F_{ma}: when parameterized with soil moisture according to Eq. (50), there is no atmospheric demand effect whatsoever represented in F_{ma}. On the other hand, when parameterized via leaf water potential according to Eq. (49), the effect of the atmosphere is also implicitly (through Ψ_v) contained in F_{ma} (De Ridder and Schayes, 1997), in addition to being represented explicitly by F_{ad}.

Consequently, four combinations of these two parameterizations are possible. The most complete combination (Eqs. (47) and (49)) represents standard PROGSURF referred to as 'Psi1'. Combination (48), (49) will be referred to as 'Psi2' (sensitivity with respect to atmospheric demand); and combination (47), (50) as 'Theta' (sensitivity with respect to moisture availability). The fourth possible combination (Eqs. (48) and (50)) has been considered irrelevant.

This architecture of PROGSURF will enable us to study the performance of LSS participating in the PILPS Phase 2(a) experiment with just one model.

4.1. Annual mean characteristics

The spinup time of Psi1, Psi2 and Theta is 2, 3 and 3 yr, respectively. The annual mean sensible and latent heat fluxes obtained by these three PROGSURF modes and the land-surface schemes participating in PILPS Phase 2(a) have been presented in Fig. 4. Deviation of a modeled point in the diagram from the observed net radiation line indicates an error in the T_{vg}-prediction; in this sense, neither Psi1 nor Psi2 nor Theta is exact. On the other hand, the results of Psi1 are in much better agreement with the observations than those of Psi2 and Theta; this sug-

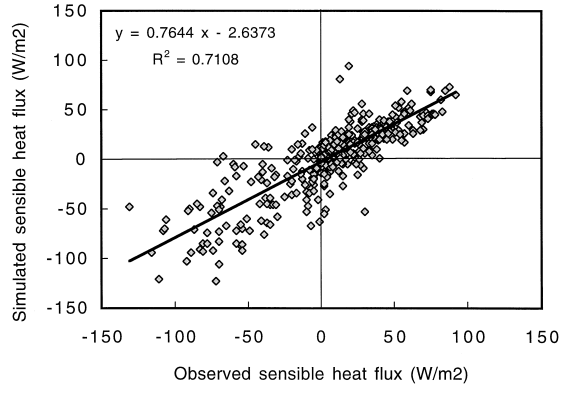

Fig. 10. Simulated (with standard PROGSURF) vs. observed sensible heat flux in the IOP.

gests that the Psi1 mode of PROGSURF represents the best parameterization.

The annual runoff vs. evapotranspiration has been presented in Fig. 5. The results of Psi1 and Psi2 are closer to the observation than those of Theta. For evapotranspiration, Psi2 overcalculates and Psi1 and Theta undercalculate the observed evapotranspiration.

The annual mean of soil water in the root zone obtained by Psi1, Psi2 and Theta is 344, 329 and 355 mm, respectively (see also Fig. 14); the corresponding estimated annual mean is about 350 mm (Chen et al., 1997).

4.2. Seasonal changes of water balance components

The monthly water balance is:

$$P_j + E_j + Q_{\mathrm{run},j} = \Delta\Theta_j \qquad (51)$$

with j as month index. P, E and Q_{run} is the monthly sum of precipitation, evapotranspiration and total runoff, respectively. Total runoff is the sum of the surface runoff Q_{runs}, subsurface lateral flows Q_{run1}, Q_{run2}, Q_{run3} and gravitational drainage Q_3. $\Delta\Theta$ is the change in total soil water (defined as $[\theta_1 + \theta_2 + \theta_3] \cdot 10$ m) storage from the start to the end of the month.

Precipitation is not presented in the following (Chen et al., 1997). The annual course of E and Q_{run} obtained by the PROGSURF modes is presented in Figs. 11 and 12. Fig. 11 shows strong seasonal changes of evapotranspiration. Note that at the specific site of Cabauw veg is quite close to unity, i.e., evapotranspiration is practically equal to transpiration. Psi2-, Psi1- and Theta-PROGSURF shows the greatest, the medium and the smallest annual amplitude, respectively. The differences in evapotranspiration between the modes are most pronounced in summer with maximum in July. Psi1 and Psi2 tend to overestimate (with maximum overestimate of 30 mm/month for Psi2), Theta to underestimate the absolute value of evapotranspiration with respect to observation. Between about October and March, the evapotranspiration obtained by Psi2 is in better agreement with the observation than those obtained by Psi1 and Theta. This result is obtained despite the missing explicit parameterization of air temperature and humidity stress in Psi2 and suggests that the implicit parameterization of Psi2 is sufficient in the cold season.

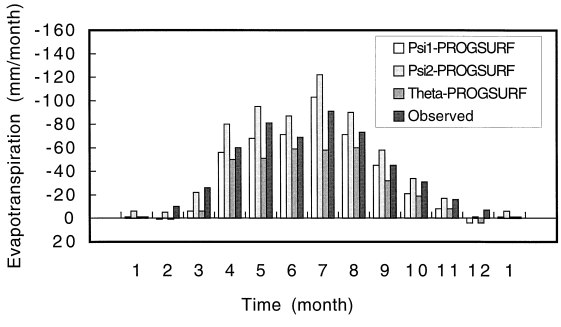

Fig. 11. Annual course of evapotranspiration simulated by the different modes of PROGSURF. Key for Psi1, Psi2, Theta as explained in Fig. 4.

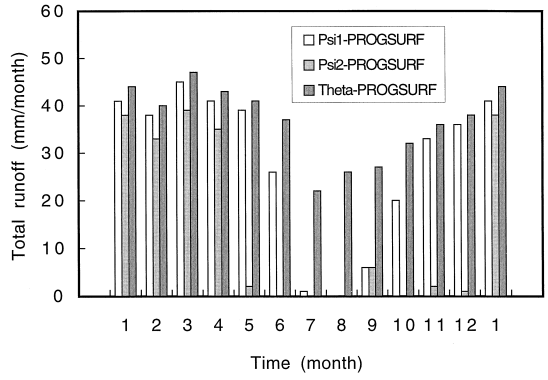

Fig. 12. As in Fig. 11 but for total runoff.

The annual course of modelled runoff for the three PROGSURF runs (observations do not exist) is reproduced in Fig. 12. Over most of winter (months 1–4) Q_{run} is between 35 and 45 mm/month, about the same for all three modes. In all other months Psi2 runs close to zero whereas Psi1 and Theta show sizeable values; for example, Psi1 and Theta yield about 30 and 40 mm/month in autumn which is more realistic than Psi2. On the other hand, Theta seems to overestimate runoff as compared to Psi1 in summer according to Chen et al. (1997).

The next two figures are for the annual course of soil water change and root-zone soil water. Soil water change in total soil depth (0–10 m) is extreme in April and October (Fig. 13). In April, the soil

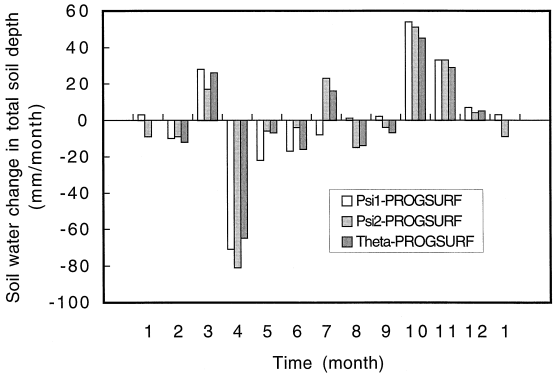

Fig. 13. As in Fig. 11 but for soil water change in total soil depth.

water decreases; in October, the situation is reversed. The changes of Theta are smaller than those of Psi1 and Psi2. In summer the change is quite variable for all three modes of PROGSURF.

The annual course of soil water in the root-zone ($\theta_1 + \theta_2$, layers 0–1 m, see Fig. 1) is presented in Fig. 14. Psi1 yields values between about 280 and 390 mm. This is in accord with the other PILPS estimates (see Fig. 15 in the paper of Chen et al., 1997).

4.3. Evapotranspiration / soil moisture relationship

Most of the physics put into the parameterizations of PROGSURF is reflected in the function $E(\theta)$ as given by Eq. (19). This function (including the factor L) is for the three PROGSURF-modes drawn in Fig. 15.

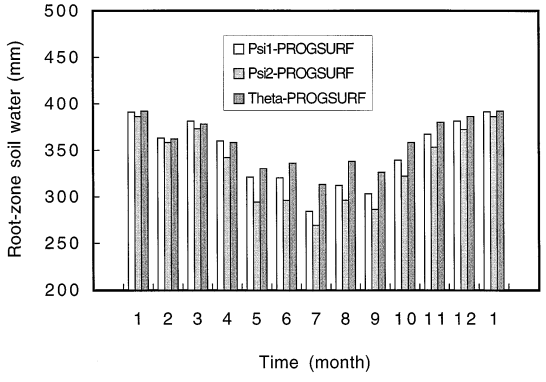

Fig. 14. As in Fig. 11 but for root-zone soil water.

Qualitatively, the two governing parameters of the $E(\theta)$-curve are the slope $S = \partial E(\theta)/\partial\theta$ in the transition region and the saturation value $E(\theta_S)$; at Cabauw $\theta_S = 0.468\ \mathrm{m^3/m^3}$. S is controlled by the parameterization of F_{ma}, $E(\theta_S)$ is controlled by the parameterization of F_{ad}.

Evidently, for low values of θ (dry surface) the evapotranspiration $E(\theta)$ is independent upon both S and $E(\theta_S)$. For extremely high values of θ (well-watered surface), it is only dependent upon $E(\theta_S)$. The influence of both parameters S and $E(\theta_S)$ upon $E(\theta)$ is maximum in the transition zone in between.

Fig. 14 has shown that the soil moisture in summer for the Cabauw data is between about 0.27 and 0.34 $\mathrm{m^3/m^3}$; i.e., it is located on the well-watered side of the transition zone of Fig. 15. Note that root zone soil *moisture* (abscissa of Fig. 15) and root zone soil *water* (ordinate of Fig. 14) are proportional. Thus, in summer, evapotranspiration is greatest for Psi2, medium for Psi1 and smallest for Theta. This, together with the fact that evapotranspiration in winter is quite low for all PROGSURF modes, explains the result found above in Fig. 11 for the annual amplitudes of the PROGSURF runs. In other words, the evapotranspiration for the Cabauw data set is predominantly controlled by the parameter $E(\theta_S)$; the parameter S is of minor influence at the Cabauw site.

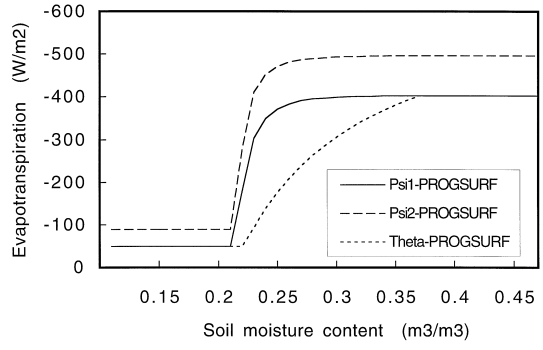

Fig. 15. Evapotranspiration vs. root zone soil moisture simulated by the different modes of PROGSURF (key for Psi1, Psi2, Theta explained in Fig. 4). Soil vegetation parameters are from the Cabauw data set. The following atmospheric conditions were kept fixed in all three runs: global radiation 800 $\mathrm{W/m^2}$; air temperature, vapor pressure and wind velocity at reference level 25.8°C, 18.0 hPa and 6.0 m/s, respectively; and precipitation zero.

This consideration demonstrates, independent upon the specific Cabauw data set, that the parameterization becomes most critical when the actual soil moisture interval happens to be located in the maximum slope part of the transition zone (this would be, for example, the interval $\theta = 0.21–0.27\ m^3/m^3$ in Fig. 15). For these cases the parameter S becomes the controlling quantity.

5. Conclusion

The prognostic land-surface flux model PROGSURF has been documented. Core of the model is a two-layer soil temperature prediction scheme based on the force-restore method plus a three-layer diffusion type soil moisture prediction scheme representing a model with four layers. The turbulent heat fluxes are parameterized by aerodynamic formulae; the aerodynamic resistance is calculated using Monin–Obukhov's similarity theory. Evapotranspiration is calculated with the surface resistance concept. The canopy surface resistance is parameterized using Jarvis' multiplicative formula. This implies specification of two governing relative conductances: one describing the atmospheric demand F_{ad} and one describing the moisture availability F_{ma}; the latter has been parameterized via leaf water potential Ψ_v.

PROGSURF has been tested in off-line mode for the Cabauw data set, using the same specifications that have been applied in the PILPS campaign (Chen et al., 1997). The standard model reproduces satisfactorily both the observed annual mean values and the seasonal changes of energy and water fluxes and root zone soil moisture content. For example, the annual mean values of evapotranspiration and runoff are -449 and 326 mm, respectively.

The model sensitivity to the canopy surface resistance formulation has also been tested by comparing the standard PROGSURF parameterization Psi1 with two modified versions (Psi2, Theta). These have been specified by changing the parameterizations of atmospheric demand and of moisture availability.

The sensitivity experiments of this study (notably Cabauw) have been made with the formal PILPS specifications; further, the Psi1-, Psi2-, Theta-experiments have been conducted with conventions similar to those of PILPS Phase 1. Thus the present study can be considered a skeleton run to qualify PROGSURF as PILPS-tested model.

The main result of the sensitivity experiments has been that the $L \cdot E(\theta)$-curve is governed by two independent parameters: the slope in the transition region and the evapotranspiration value in the saturated region. The slope is controlled by the parameterization of moisture availability, the saturation value is controlled by the parameterization of atmospheric demand. For the Cabauw data, the saturation value has been of prominent relevance since the actual moisture at Cabauw in summer is located on the well-watered side of the transition region. With these results we have explained the differences in the annual evapotranspiration (and thus, of the runoff and of the other water balance components) values of the three PROGSURF modes.

In addition to that, our tests suggest that the considerable scatter in the results of the other PILPS models is caused by the two parameters of the $L \cdot E(\theta)$-curve just discussed. Differences in the parameterization of atmospheric demand and of moisture availability may be the ultimate cause for the differences between the various PILPS models as presented by Chen et al. (1997) and reproduced in our Figs. 4 and 5.

Further investigations of the mechanisms discussed here are needed. It is hoped that the further intercomparison campaigns presently in preparation may be useful in optimizing evapotranspiration parameterization in land-surface schemes. PROGSURF is presently used to specify the boundary conditions (as substitute for observed fluxes of latent and sensible heat) for the software DIAMOD (Haimberger et al., 1995) which is routinely used at the University of Vienna to diagnose the convective fluxes in the free atmosphere.

Acknowledgements

The *Österreichische Akademie der Wissenschaften* gave financial support for this study within the National Austrian Committee for the IGBP. We thank M. Dorninger, L. Haimberger and F. Hamelbeck for fruitful discussions and invaluable help in data handling. Mr. Z. Barcza and Mrs. B. Berger provided technical assistance.

References

Ács, F., 1994. A coupled soil–vegetation scheme description, parameters, validation, and sensitivity studies. J. Appl. Meteorol. 33, 268–284.

Ács, F., Mihailovic, D.T., Rajkovic, B., 1991. A coupled soil moisture and surface temperature prediction model. J. Appl. Meteorol. 30, 812–822.

Beljaars, A.C.M., Bosveld, F.C., 1997. Cabauw data for the validation of land-surface parameterization schemes. J. Climate 10, 1172–1194.

Bhumralkar, C.M., 1975. Numerical experiments on the computation of ground surface temperature in an atmospheric general circulation model. J. Appl. Meteorol. 14, 1246–1258.

Chen, T.H., Henderson-Sellers, A., Milly, P.C.D., Pitman, A.J., Beljaars, A.C.M., Polcher, J., Abramopoulos, F., Boone, A., Chang, S., Chen, F., Dai, Y., Desborough, C.E., Dickinson, R.E., Dümenil, L., Ek, M., Garratt, J.R., Gedney, N., Gusev, Y.M., Kim, J., Koster, R., Kowalczyk, E.A., Laval, K., Lean, J., Lettenmaier, D., Liang, X., Mahfouf, J.F., Mengelkamp, H.T., Mitchell, K., Nasonova, O.N., Noilhan, J., Robock, A., Rosenzweig, C., Schaake, J., Schlosser, C.A., Schulz, J.P., Shao, Y., Shmakin, A.B., Verseghy, D.L., Wetzel, P., Wood, E.F., Xue, Y., Yang, Z.L., Zeng, Q., 1997. Cabauw experimental results from the project for intercomparison of land-surface parameterization schemes. J. Climate 10, 1194–1216.

Choudhury, B., 1983. Simulating the effects of weather variables and soil water potential on a corn canopy temperature. Agric. Meteorol. 29, 169–182.

Clapp, R.B., Hornberger, G.M., 1978. Empirical equations for some soil hydraulic properties. Water Resour. Res. 14, 601–604.

De Ridder, K., Schayes, G., 1997. The IAGL land-surface model. J. Appl. Meteorol. 36, 167–183.

Dickinson, R.E., 1984. Modelling evapotranspiration for three dimensional global climate models. In: Hanson, J.E., Takahashi, T. (Eds.), Climate Processes and Climate Sensitivity, Vol. 29 of Geophys. Monogr., Am. Geophys. Union, pp. 58–72.

Dolman, A., 1993. A multiple-source land-surface energy balance model for use in general circulation models. Agric. Meteorol. 65, 21–45.

Entekhabi, D., Eagleson, P.S., 1989. Land-surface hydrology parameterization for atmospheric general circulation models including subgrid scale spatial variability. J. Climate 2, 816–831.

Gates, M.D., 1981. Biophysical Ecology. Springer, 339 pp.

Gerwitz, A., Page, E.R., 1974. An empirical mathematical model to describe plant root system. J. Appl. Ecol. 11, 773–782.

Haimberger, L., Hantel, M., Dorninger, M., 1995. A thermodynamic model for the atmosphere: Part III. DIAMOD with orography and improved error model. Meteorol. Z., N.F. 4, 162–182.

Henderson-Sellers, A., 1996. Soil moisture simulation: achievements of the RICE and PILPS intercomparison workshop and future directions. Global Planet. Change 13, 99–115.

Henderson-Sellers, A., Yang, Z.L., Dickinson, R.E., 1993. The project for intercomparison of land-surface parameterization schemes. Bull. Am. Meteorol. Soc. 74, 1335–1349.

Henderson-Sellers, A., Pitman, A.J., Love, P., Irannejad, P., Chen, T., 1995. The project for intercomparison of land-surface parameterization schemes (PILPS): phases 2 and 3. Bull. Am. Meteorol. Soc. 76, 489–503.

Idso, S., Jackson, R., Reginato, R., Kimball, B., Nakayama, F., 1975. The dependence of bare soil albedo on soil water content. J. Appl. Meteorol. 14, 109–113.

Jarvis, P.G., 1976. The interpretation of the variations in leaf water potential and stomatal conductance found in canopies in the field. Philos. Trans. R. Soc. London, Ser. B 273, 593–610.

Kondratjev, K.Y., Korzov, V.I., Mukhenberg, V.V., Dyachenko, L.N., 1982. The shortwave albedo and the surface emissivity. In: Eagleson, P.S. (Ed.), Land-surface Processes in Atmospheric General Circulation Models. Cambridge Univ. Press, pp. 463–514.

Lynn, B.H., Carlson, T.N., 1990. A stomatal resistance model illustrating plant vs. external control of transpiration. Agric. For. Meteorol. 52, 5–43.

McCumber, M.C., Pielke, R.A., 1981. Simulation of the effects of surface fluxes of heat and moisture in a mesoscale numerical model: Part I. Soil layer. J. Geophys. Res. 86, 9929–9938.

Mihailović, D.T., 1996. Description of a land–air parameterization scheme (LAPS). Global Planet. Change 13, 207–215.

Monteith, J., 1965. Evaporation and environment. In: Fogg, G. (Ed.), The State and Movement of Water in Living Organisms. Proc. 19th Symp. Soc. Exp. Biol., Cambridge. Cambridge Univ. Press, pp. 205–236.

Monteith, J., 1995. Accommodation between transpiring vegetation and the convective boundary layer. J. Hydrol. 166, 251–263.

Noilhan, J., Planton, S., 1989. A simple parameterization of land-surface processes for meteorological models. Mon. Wea. Rev. 117, 536–550.

Pielke, R.A., 1984. Mesoscale Meteorological Modeling. Academic Press.

Schlosser, C.A., Robock, A., Pitman, A.J., Slater, A., Entin, J., 1997. Preliminary results from PILPS phase (2d): analysis of modeled soil–water and snow processes for an 18-year period at a midlatitude grassland catchment. Proceeding of the Joint Assemblies of IAMAS and IAPSO. Melbourne, Australia, July 1–10, 1997.

Sellers, P.J., Dorman, J.L., 1987. Testing the simple biosphere model (SiB) using point micrometeorological and biophysical data. J. Clim. Appl. Meteorol. 26, 622–651.

Sellers, P.J., Mintz, Y., Sud, Y.C., Dalcher, A., 1986. A simple biosphere model (SiB) for use within general circulation models. J. Atmos. Sci. 43 (7), 505–531.

Shao, Y., Henderson-Sellers, A., 1996. Validation of soil moisture simulation in land-surface parameterization schemes with HAPEX data. Global Planet. Change 13, 11–46.

Shuttleworth, W.J., Wallace, J.S., 1985. Evaporation from sparse crops—an energy combination theory. Q. J. R. Meteorol. Soc. 111, 839–855.

van der Hornert, T.H., 1948. Water transport as a catenary process. Discuss. Faraday Soc. 3, 146–153.

Xue, Y., Zeng, F.J., Schlosser, C.A., 1996. SSiB and its sensitivity to soil properties—a case study using HAPEX–Mobilhy data. Global Planet. Change 13, 183–194.